Annals of Phytomedicine 10(2): 72-81, 2021

DOI: http://dx.doi.org/10.21276/ap.2021.10.2.10

Annals of Phytomedicine: An International Journal

http://www.ukaazpublications.com/publications/index.php

Print ISSN : 2278-9839 Online ISSN : 2393-9885

Original Article : Open Access

An attempt to increase efficacy of doxorubicin against MCF-7 cells by using nanotechnology

M.D. Imad Uddin◆* and B. Veeresh**

Department of Pharmacology, Pulla Reddy Institute of Pharmacy, Hyderabad-502313, Telangana State, India

**Department of Pharmacy, University College of Technology, Osmania University, Hyderabad-500007, Telangana State, India*

***Department of Pharmacology, G. Pulla Reddy College of Pharmacy, Hyderabad-500028, Telangana State, India*

Article Info

Article history

Received 10 October 2021

Revised 27 November 2021

Accepted 29 November 2021

Published Online 30 December 2021

Keywords

Chitosan

FTIR

Particle size

Zetapotential

SEM

MTT assay

Anticancer activity

Abstract

This research is conducted to increase the therapeutic efficacy of the commonly used anticancer drug doxorubicin (DRN), commonly called Adriamycin. The most popular mechanisms of DRN are inhibiting the topoisomerase-II enzyme and forming a complex with DNA. A major challenge in the use of this drug is severe cardiotoxicity, immunotoxicity, and the development of multidrug resistance. Nanotechnology is applied to overcome all these problems. This research is conducted with the idea to incorporate DRN in chitosan nanoparticles (NPs). DRN was found to have the highest solubility in water and λmax was found to be 232 nm. Major FTIR peaks of chitosan, STTP, pure DRN, physical mixture of chitosan-STTP, and physical mixture of DRN-chitosan-STTP represented their respective functional groups in each spectrum. To optimize the concentration of chitosan, STTP, and DRN for preparing NPs, a range of plain chitosan NPs (PLN-CNPs) and DRN loaded chitosan NPs (DRN-CNPs) are prepared. The polydispersity index (PDI), particle size, zeta potential, and electrophoretic mobility mean (EMM) is measured for all these formulations. Pareto analysis of particle size and PDI showed PLN-CNPs-3 and DRN-CNPs-1 as the best formulations for further studies. FTIR analysis of PLN-CNPs-3 and DRN-CNPs-1 showed the functional groups which represent cross linking of chitosan and STTP and incorporation of DRN in NPs, respectively. SEM analysis showed the particle size as 172 nm and 174 nm for PLN-CNPs-3 and DRN-CNPs-1 NPs. DRN-CNPs are further evaluated for release of the drug, encapsulation, and loading efficiency. After 60 h, more than 50% of the drug was released from the formulation. Encapsulation efficiency, loading efficiency, and % yield of DRN-CNPs-1 were found to be 78.5%, 13.8%, and 35.7%, respectively. Debye-Scherrer equation was applied for 2θ peaks obtained from XRD data of DRN-CNPs-1 to calculate average particle size (30.50 nm). Anticancer activity of DRN-CNPs-1 was compared with unloaded DRN against MCF-7 cell lines. It was dose dependent in both treatments and DRN-CNPs-1 was found to be more effective than DRN. This research put forth an idea to use chitosan a biocompatible polymer for loading anticancer drugs like DRN to increase their efficacy.

1. Introduction

Cancer is a dreadful disease, characterized by the development of benign or malignant tumors from the cells which escape the normal death process and continue to divide without control. It is of many types based on location and based on pathophysiology. It was first identified in the 16th century and was considered a challenging disease to mankind around the world and till the 19th century, no cure was identified for cancer (Han *et al*., 2006).Till the middle of the 19th century, surgery was considered as the first line of treatment for many types of cancer, but later on discovery of nitrogen mustard laid the path for chemotherapeutic treatment (Papac, 2001). By considering financial and social burden of cancer on humanity research around the world focused on discovering various modes of treatment. Cryotherapy, chemotherapy, hormonal therapy radiation therapy, and gene therapy are some of the commonly discovered advanced modes of treatment for cancer (American Cancer Society, 2019). Despite many treatment options, cancer mortality remains a challenge. According to the WHO, cancer fact sheet dated 21 September 2021, about 1 crore people around the world died due to different types of cancer in 2020. Breast cancer was found to be most prevailing type with 22.6 lakh new cases in 2020 (World Health Organization, 2021). Similarly, lung cancer was also found to be prevailing at the same rate as that of breast cancer, *i.e.*, affecting around 22.1 lakh people in 2020. Therefore, cancer remains a major challenge to be addressed in the healthcare system and specifically with an emergency call of breast and lung cancer management.

DRN is a well-known anticancer drug belonging to the anthracycline family (Prados, 2012). DRN is widely used as a first-line drug for treatment of breast cancer. It acts by blocking the topoisomerase-II enzyme. As this enzyme is inhibited DRN successfully blocks DNA replication. It also acts by getting intercalated into DNA. Thus, by these two mechanisms, it is successfully producing antimitotic and cytotoxic activity by inhibiting gene expression and producing oxidative stress in the form of generation of reactive oxygen species (Chatterjee, 2010). A major challenge in use of DRN is the development of drug resistance. Apart from this, it is also presented with

Corresponding author: Mr. M.D. Imad Uddin

Associate Professor Department of Pharmacology, Pulla Reddy Institute of Pharmacy, Hyderabad-502313, Telangana State, India

E-mail: imadpharma111@gmail.com

Tel.: +91-8374175556

severe cardiac related problems, bone marrow related abnormalities, and attacking normal cells along with cancer cells. These all problems should be addressed to increase the use of this established anticancer drug. The discovery of nanotechnology appeared as a boon for the treatment of many diseases.

For a few decades, researchers throughout the world showed a keen interest in nanotechnology. Different types of NPs like inorganic NPs, *e.g*., quantum dots, gold NPs, *etc*., organic NPs, e.g: dendrimers, micelles, *etc*., and hybrid NPs, e.g: lipid-polymer hybrid NPs, *etc*., are reported to improve anticancer activity of different chemo-therapeutic agents (Yao *et al*., 2020). Requirement of low dose, targeted delivery and increased bioavailability are some of the important benefits of using NPs loaded drug delivery systems (Zhang *et al*., 2016). Poly (lactide-co-glycolide), poly (lactide), alginate, albumin, chitosan is some of the commonly used polymers for preparation of NPs. Therefore, this research was carried out in an attempt to optimize the best suited concentration of chitosan and STTP for the synthesis of DRN loaded NPs. These DRN NPs are evaluated for their anticancer efficacy against MCF-7 cells.

2. Materials and Methods

2.1 Chemicals and cell lines

Chitosan was used as a polymer for loading DRN, obtained from Vihan life sciences, Ahmednagar, India. A cross linker sodium tripolyphosphate, sodium hydroxide, and hydrochloric acid were obtained from SD Fine Chemicals Limited, Mumbai, India. Doxorubicin-an anticancer drug was obtained from Sigma Aldrich, Icon Biosystems, Hyderabad, India. Breast cancer cell line MCF-7 cells were obtained from the National Center for Cell Sciences (NCCS), Pune.These MCF-7 cells are cultured according to the standard protocol as follows. These cells are cultured in a minimum essential medium containing a higher concentration of essential nutrients. An experiment was carried out at 37°C and used 5% of CO_2.

2.2 Methods

2.2.1 Characterisation of DRN

DRN procured was further characterized by using different techniques. A saturated solubility study was conducted by using the shake flask method with different solvents, *viz*., distilled water, DMSO, ethanol, 0.1M HCl, 0.1M H_2SO_4, 6.8, and 8.4 PBS. About 2 ml of each solvent was taken in a glass vial. After adding an excess amount of drug to each solvent, mouth was closed. These closed vials are shaken on an orbital shaking incubator for 48 h equipment was set to rotate at 50 rpm and maintained at a temperature of 37°C. At the end of 48 h, solution is centrifuged and the clear supernatant was collected. This is diluted further in the respective solvent system and absorption was taken by using UV-visible spectroscopy at solvent respective λmax. Finally, absorption of drug is converted to concentration by using standard curve of DRN in the respective solvent.

λmax of DRN was estimated by measuring absorption on UV spectroscopy (Lab India-UV3000) operated in the range of 200-600 nm. Later on, about 10 ml of DRN stock solution of concentration 1 mg/ml is produced in distilled water. By using this stock solution, 3, 6, 9, 12, and 15 µg/ml solutions are prepared which are used to obtain a calibration curve at 232 nm. For FTIR analysis, a minute quantity of DRN was taken in a microspatula and 0.40 teaspoons of KBr was added. This was mixed thoroughly by using motor and pestle. This mixture is pressed at 5000-10000 psi to obtain a pellet. This pellet was analysed for the presence of functional groups by using an FTIR spectrophotometer (Bruker, Alpha) operated in the range from 4000 to 500 cm^{-1}. In addition to DRN, FTIR analysis was also carried out for chitosan, STTP, physical mixture of chitosan and STTP; DRN, chitosan and STTP. The melting point was measured by using the capillary tube method. DRN was taken up to a height of 3 mm in one side closed capillary tube. This capillary tube is placed in melting point apparatus (Bio Technics, India) to analyze the sample.

2.2.2 Synthesis and characterization of PLN-CNPs and DRN-CNPs

2.2.2.1 Synthesis of PLN-CNPs and DRN-CNPs

25 ml of low molecular weight chitosan solution (0.5 mg/ml) was prepared by dissolving 12.5 mg of chitosan in 25 ml of 1% acetic acid and pH was adjusted to 4.7 by adding 1M NaOH solution. Similarly, 25 ml of STPP solution (0.7 mg/ml) was prepared by dissolving 17.5 mg of sodium tripolyphosphate (STTP) in 25 ml of distilled water, and pH was adjusted to 2 using 1M HCl.

In this study, to optimize the best suited concentration of chitosan, STTP, and DRN for preparing NPs, a range of PLN-CNPs and DRN-CNPs are prepared. Both of these NPs are prepared by a slight modification of the ionic gelation method reported by Othman *et al*. (2018). Five different formulations, 1, 2, 3, 4, and 5 of PLN-CNPs were prepared by adding 600 µl of chitosan solution to 100, 200, 300, 400 and 500 µl of STPP solution, respectively. DRN-CNPs were prepared in two steps: In the first step, the range of DRN-STTP solutions (formulation 1, 2, and 3) were prepared by adding 500, 1000, and 1500 µg/ml of DRN to 300 µl of above prepared STTP solution, respectively. In the second step, 600 µl of chitosan was added to the above prepared DRN-STTP solutions to make DRN loaded CNPs.

2.2.2.2 Particle size, PDI, zeta potential and EMM estimation of PLN-CNPs and DRN-CNPs

PDI, particle size and stability of solution (zeta potential) were determined for all the above prepared PLN-CNPs (formulation 1 to 5) and DRN-CNPs (formulation 1 to 3) by using Horiba-SZ-100 zeta sizer. For measurement of particle size and PDI instrument was operated with scattering angle of 90°C, the temp of holder was 25°C, the viscosity of dispersion medium was 2.035 mPa.s, representation of result by scattering light intensity method, and count rate was 342 kCPS. Whereas for measurement of zeta potential and EMM, zeta sizer was operated with a temperature of the holder at 25°C, the viscosity of dispersion medium was 0.893 mPa.s, conductivity was 0.221 mS/cm, and electrode voltage was 3.3 V. All these data of particle size and PDI are analyzed by Pareto analysis in Microsoft excel-2019 to obtain the best formulation for further study. The best selected formulation is further analysed by FTIR and SEM analysis.

2.2.2.3 FTIR and SEM analysis of PLN-CNPs and DRN-CNPs

Functional groups present in these PLN-CNPs and DRN-CNPs were determined by FTIR analysis (Shimadzu-8400S). FTIR spectrometer

was operated with a working range of 4000 to 500 cm^{-1}, no. of scans was 10, a resolution was 4 cm^{-1} and apodization was done by square triangle method. Morphological features of PLN-CNPs and DRN-CNPs were determined by using a scanning electron microscope (SEM) (Hitachi-S3700N) operated at a magnification of 2 K to 8 K, acceleration voltage of 30 KV, emission current of ~ 100000 nA, and working distance of 9.1 to 9.2 mm. Best selected DRN-CNPs are further characterized for *in vitro* drug release efficiency, encapsulation efficiency, loading efficiency, XRD analysis.

2.2.3 *In vitro* drug release, encapsulation efficiency, loading efficiency, and % yield estimation of DRN-CNPs

For evaluating *in vitro* drug release, 10 mg of DRN-CNPs was suspended in 1000 µl of PBS (pH=7.4).This suspension was taken in a dialysis bag (cut-off molecular weight of dialysis membrane was 10000 – 12000 Da). The bag was immersed in a 5 ml PBS (pH=7.4) and incubated at 37°C. At 0, 20, 40, 60, 80 and 100 h about 5 ml of release medium was withdrawn and 5 ml of fresh PBS was added. The amount of drug released in the medium was estimated at 232 nm by using UV *Vis* spectrophotometer. For screening encapsulation efficiency, loading efficiency, 1ml of DRN-CNPs is centrifuged. The absorbance of the supernatant was obtained at 232 nm. Formulas used as follows:

$$EE\% = \left(\frac{\text{Total drug used for NP preparation - Free drug present}}{\text{Total drug used for NP preparation}}\right) \times 100$$

$$LE\% = \left(\frac{\text{Total drug used for NP preparation - Free drug present}}{\text{Yeild of NPs}}\right) \times 100$$

$$\%\text{Yield of NPs} = \left(\frac{W_1}{W_2}\right) \times 100$$

where as W_1 = Dried Wt. of NP's, W_2 = Wt. of drug + Wt. of STPP + Wt. of Chitosan.

2.2.4 XRD analysis of DRN-CNPs

To identify the phase and to assess the crystallographic structure of the purified DRN-CNPs, XRD studies were carried out. XRD instrument was operated at a voltage of 40 kV and a current of 30 mA with Kα1 Cu radiation, λ = 1.54 Å with nickel monochromator in the 2θ range from 10° to 80°. In order to carry out XRD analysis, 100 µl of DRN-CNPs was applied as a thin film on a glass slide and allowed to dry for 30 min and subjected to diffraction studies. The average size of NPs was assessed by using the Debye-Scherrer equation.

$$D = \left(\frac{K}{\beta \cos \theta}\right)$$

where D = average size of DRN-CNPs, k = constant (0.94), β = wavelength of X- rays (0.1546 Å), β = full width at half maximum, θ = diffraction angle in degrees.

2.2.5 *In vitro* anticancer activity of plain DRN and DRN-CNPs against MCF-7 cells

MCF-7 cells were plated at a density of 5 x 10^3 cells per well in a 96 well plate which was supplemented with 10% FBS. This is incubated for 24 h at 37°C and 5% CO_2. These cells were treated with vehicle, pure DRN, and DRN-CNPs for 48 h. Cell viability was determined by adding 100 µl of 3-(4,5-Dimethyl-2-thiazolyl)-2,5-diphenyl-2H-tetrazolium bromide, MTT reagent (0.5 mg/ml) dissolved in serum free media added to each well and incubated for 4 h. Then, the media was aspirated and the formazan crystals were dissolved in 200 µl of DMSO absorbance was taken at 570 nm in a multimode plate reader (BioTek Instruments, Synergy 4, Winooski, VT). The per cent cell inhibition in treated cells was calculated by normalizing the cells with 0% inhibition with the control group.

3. Results

3.1 Characterisation of DRN

A saturated solubility study was conducted by using different solvents. DRN was found to be more soluble in water followed by DMSO. Its solubility is less in pH 6.8 and pH 8.4 PBS solutions, these solutions are evidenced with precipitate formation. However, it is sparingly soluble in ethanol and both acids. The concentration of drug soluble in different solvents is represented in Table 1 as follows.

Table 1: Concentration of DRN soluble in different solvents

S.No.	Name of solvent	Concentration of DRN (µg/ml)
1.	Distilled water	48.45
2.	DMSO	40.73
3.	Ethanol	18.61
4.	0.1 M HCl	20.34
5.	0.1 M H_2SO_4	15.92
6.	PBS 6.8 pH	24.85
7.	PBS 8.4 pH	26.19

As DRN showed maximum solubility in water, it is selected as a solvent for further characterization. Žmax of DRN was found to be at 232 nm and the calibration curve was obtained with an R^2 value of 0.993 (Figure 1). In FTIR analysis, chitosan showed peaks at 3449.16, 2875.64, 1651.48, 1370.68 cm^{-1}, corresponding to N-H & O-H stretching, C-H asymmetric stretching, C=O stretching of amide-I, and C=N stretching of amide-III, respectively. STTP showed peaks at 1209.72, 1126.24, 916.55 cm^{-1}, corresponding to P=O stretching, PO2 symmetric and asymmetric stretching, P-O-P bridge antisymmetric stretching, respectively. DRN showed peaks

at 3313.10, 2890.04, 1729.31, 1281.51, 989.60 cm^{-1}, corresponding to stretching vibrations of phenolic O-H group, C-H stretching band, C=O stretching vibrations, and stretching bands of C-O-C groups, respectively. Whereas in a physical mixture of chitosan and STTP 3261.84, 1124.31, 879.65 cm^{-1}, peaks are observed. First peak 3261.84 cm^{-1} corresponds to N-H & O-H stretching of chitosan and other peaks like 1124.31, 879.65 cm^{-1} corresponds to PO2 symmetric and asymmetric stretching and P-O-P bridge antisymmetric stretching of STTP respectively (Figure 2). Similarly, in the physical mixture of DRN, chitosan and STTP, peaks corresponding to all three compounds are shown. The peak at 3259.38 cm^{-1} corresponds to N-H & O-H stretching of chitosan, peak at 2974.12 cm^{-1} corresponds to C-H stretching of DRN, and peak at 1124.12 and 875.77 cm^{-1} corresponds to PO2 symmetric and asymmetric stretching, P-O-P bridge antisymmetric stretching of STTP, respectively (Figure 3). The melting point of DRN was found to be 214°C after successful characterization of DRN, it is used for synthesis NPs.

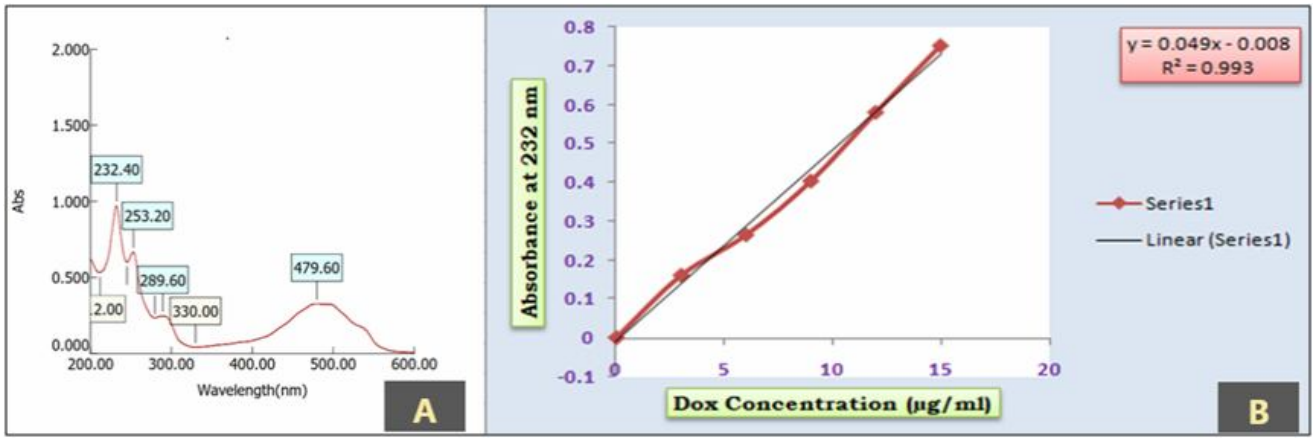

Figure 1: A-Lambda max of DRN calculated. B-Calibration curve of DRN plotted by using DRN concentration on X-axis and absorbance on Y-axis.

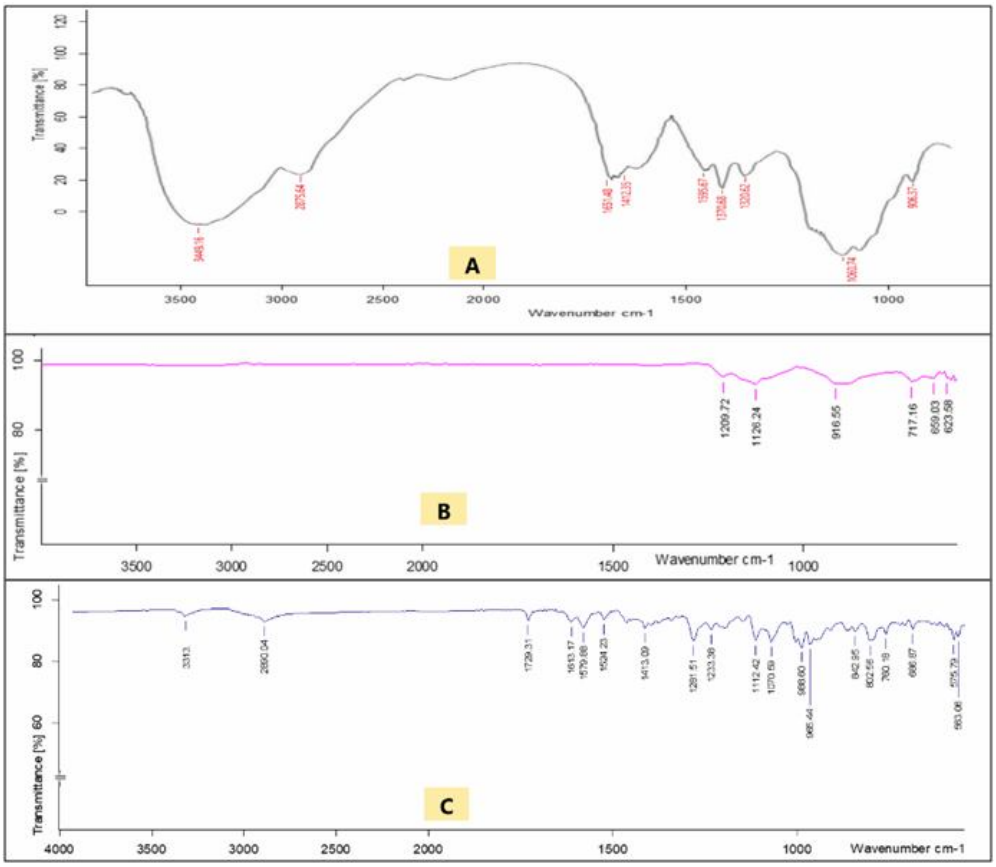

Figure 2: FTIR spectra of different compounds, A-Chitosan, B-STTP, C-DRN.

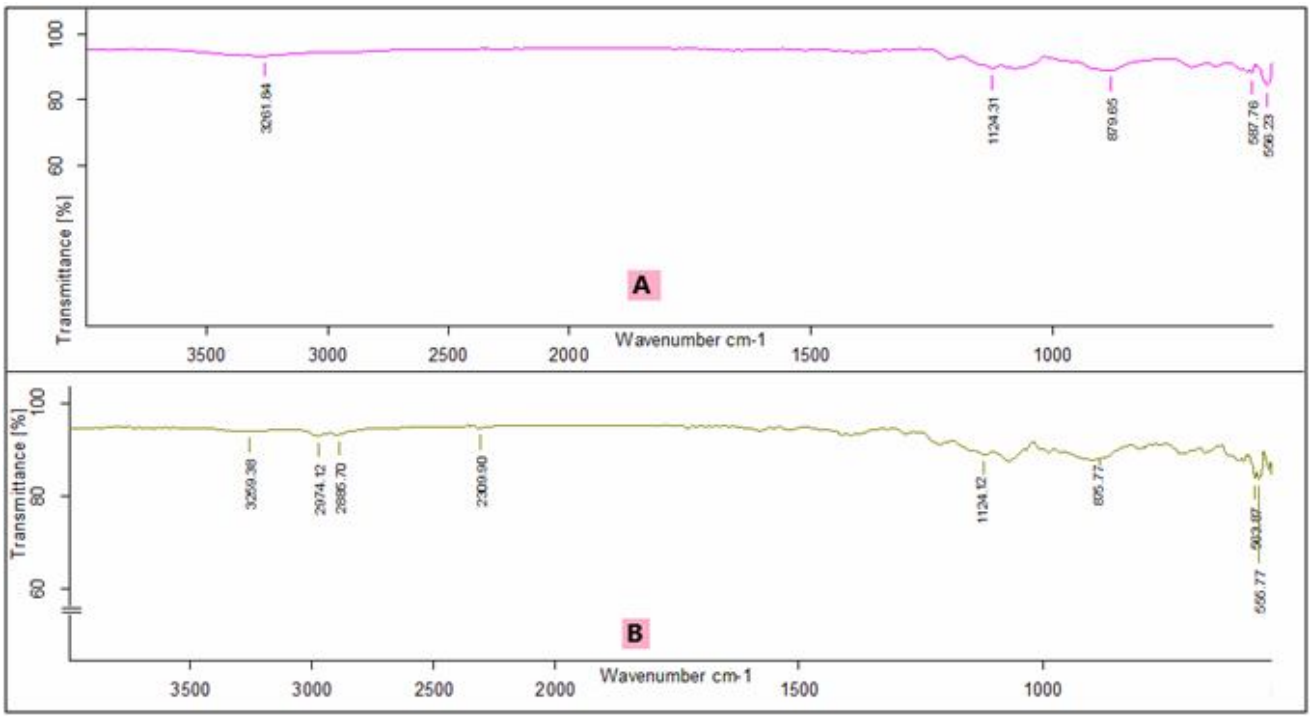

Figure 3: FTIR spectra of physical mixture of different compounds, A-Chitosan and STTP, B-DRN, chitosan, and STTP.

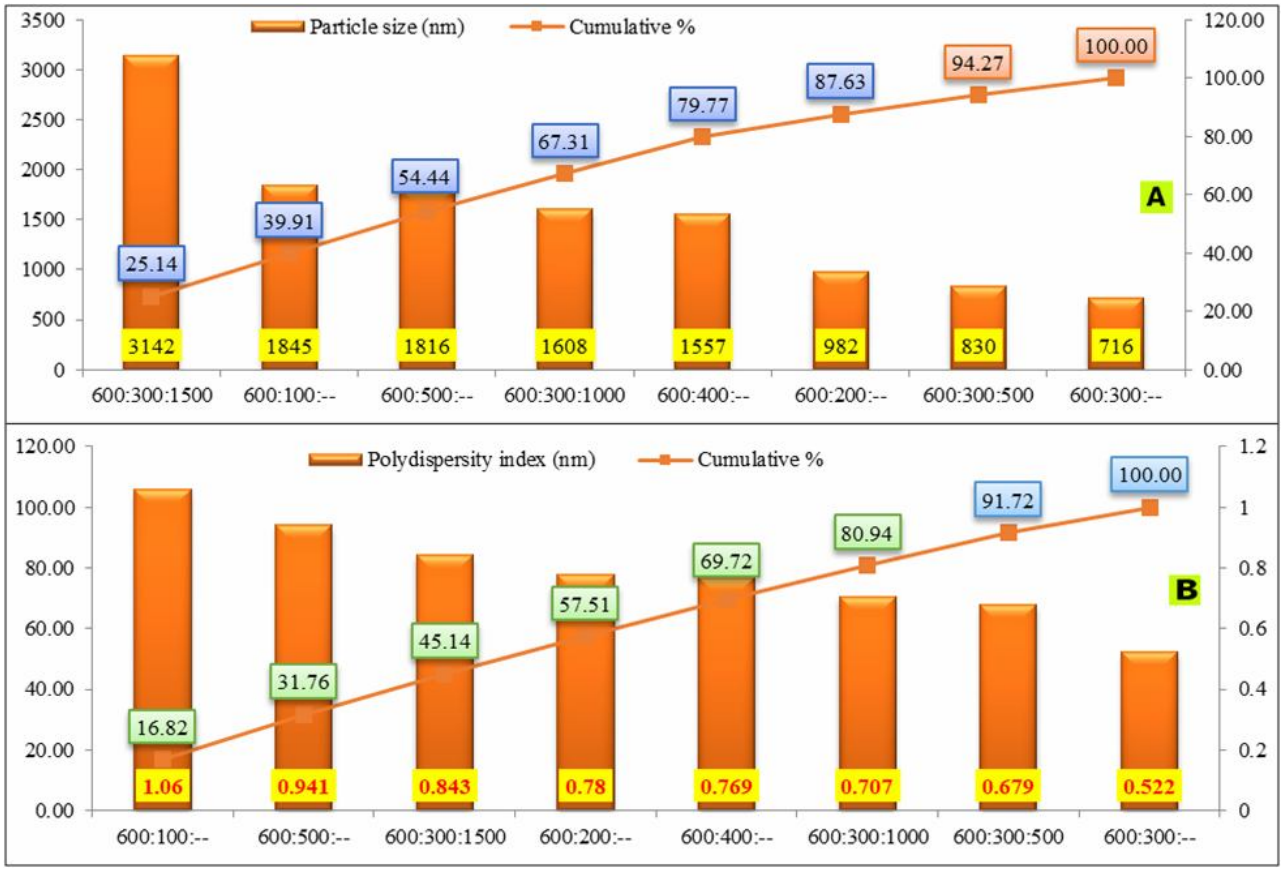

Figure 4: Pareto analysis of particle size (A) and PDI (B) of all eight formulations, formulation PLN-CNPs-3 (600:300) and DRN-CNPs-1 (600: 300:500) are selected as they are above 80 per cent.

Table 2: Particle size, PDI, zeta potential, and EMM calculated for PLN-CNPs and DRN-CNPs

Formulation	Volume of chitosan(µl): STTP(µl): DRN (µg/ml)	Particle size (nm)	PDI	Zeta potential (mV)	EMM (cm2/Vs)
PLN-CNPs - 1	600:100:–	1845	1.06	-11.9	-0.000089
PLN-CNPs - 2	600:200:–	982	0.78	-22.9	-0.000100
PLN-CNPs - 3	600:300:–	716	0.522	-41.4	-0.000124
PLN-CNPs - 4	600:400:–	1557	0.769	-26.1	-0.000097
PLN-CNPs - 5	600:500:–	1816	0.941	-28.7	-0.000112
DRN-CNPs - 1	600:300:500	830	0.679	33.4	0.000027
DRN-CNPs - 2	600:300:1000	1608	0.707	24.8	0.000015
DRN-CNPs - 3	600:300:1500	3142	0.843	18.7	0.000009

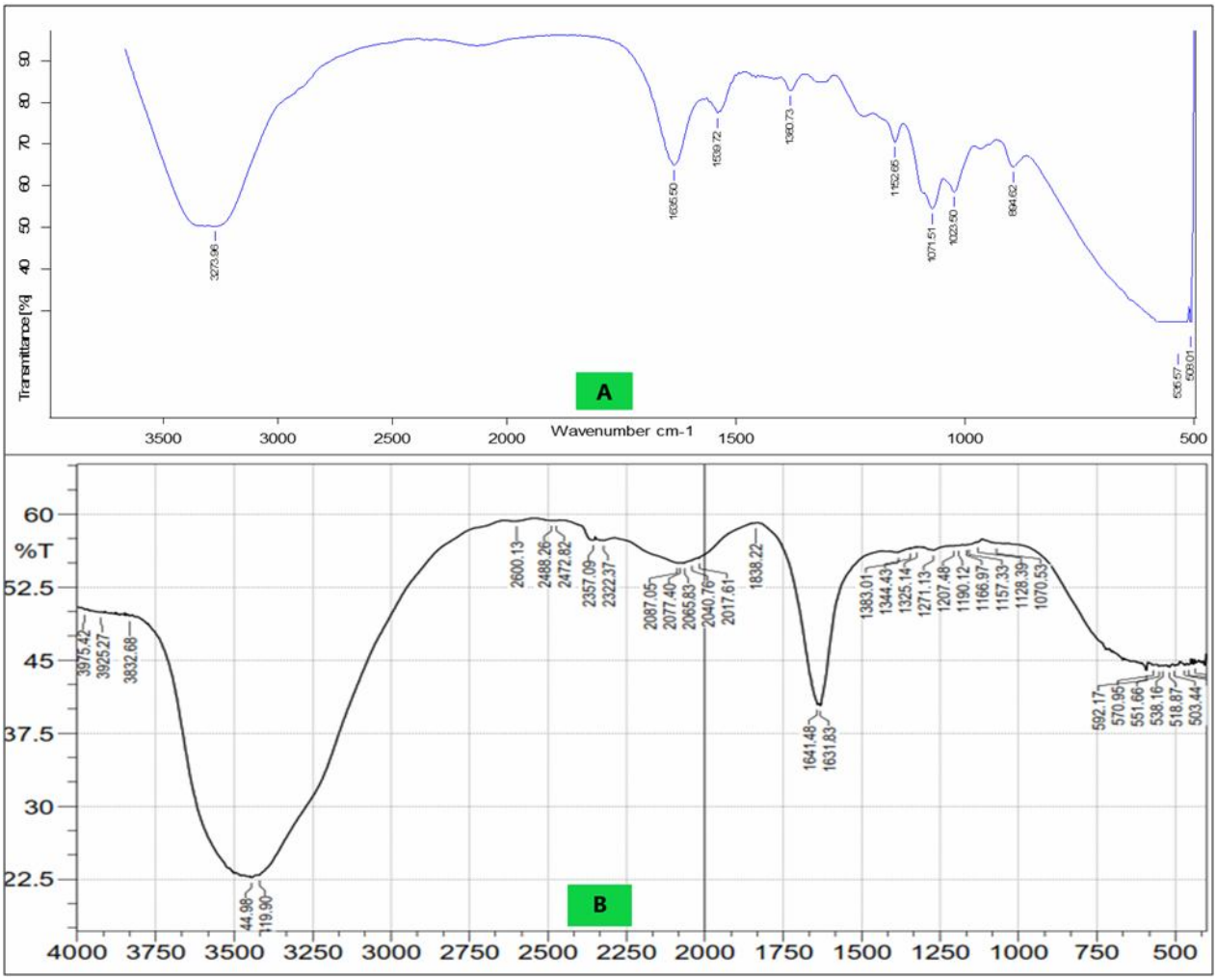

Figure 5: FTIR analysis to explore possible functional groups of various compounds. A-FTIR spectra of PLN-CNPs-3 and B-FTIR spectra of DRN-CNPs-1.

3.2 Particle size, PDI, and zeta potential estimation of PLN-CNPs and DRN-CNPs

To optimize the concentration of chitosan, STTP, and DRN for preparing NPs, a range of PLN-CNPs and DRN-CNPs are prepared. Among all five formulations of PLN-CNPs, PLN-CNPs-3 showed a particle size of 716 nm and this was increased as the volume of STTP increased in the next two formulations, *i.e.*, PLN-CNPs 4 and 5. PDI was found to be 0.522 for the third formulation and this was found to increase in the next formulations as reported with particle size. Zeta potential and EMM were found to be -41.4mV and -0.000124 cm^2/Vs for PLN-CNPs-3. Both of these parameters

increased as there was an increase in the volume of STTP added in the next formulations. Whereas DRN-CNPs are prepared with increasing concentration of DRN. As the concentration of DRN increased there was an increase in particle size and PDI and there was an increase in zeta potential and EMM. Particle size and PDI data were subjected to Pareto analysis to identify the best suited formulation for further studies. PLN-CNPs-3 and DRN-CNPs-1 were found to be the best formulations for further research (Table 2) (Figure 4).

3.3 FTIR and SEM analysis of PLN-CNPs-3 and DRN-CNPs-1

FTIR analysis of PLN-CNPs found to produce peaks at 3273.96, 1635.50, and 1539.72 cm^{-1} corresponding to C-O indicating the presence of hydrogen bonded alcohols, C=C Stretching indicating the presence of alkene, and C=C absorption band, respectively. Whereas FTIR analysis of DRN-CNPs-1 was found to produce peaks at 3444.98, 1641.48, 1157.33, 1070.53 cm^{-1} corresponding to C=O stretching of amide-I indicates the presence of N-acetyl group, C-O-C asymmetric stretching, O-H group stretching, and C=O stretching vibration, respectively (Figure 5).The average size of synthesized NPs was estimated by SEM. PLN-CNPs and DRN-CNPs were found to get an average size (range) of 172nm (129-229nm) and 174nm (146-194nm), respectively (Figure 6).

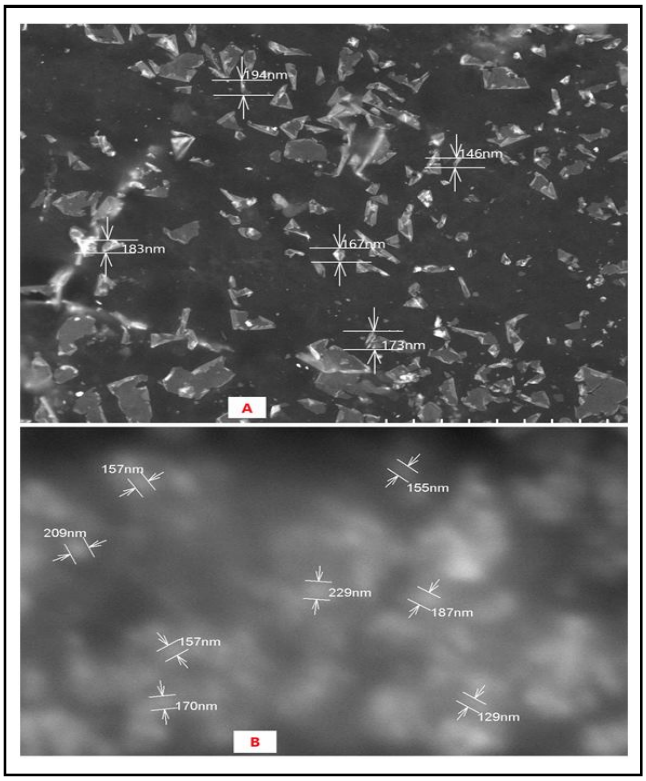

Figure 6: A-SEM image of PLN-CNPs-3, and B-SEM image of DRN-CNPs-1.

3.4 *Invitro* drug release, encapsulation efficiency, loading efficiency, % yield, XRD analysis, and *in vitro* anticancer activity of DRN-CNPs:

DRN-CNPs are evaluated for % release of drug at different time points as mentioned above. At 20 h 15.92% of the drug was released and it increased up to 65.47% by 100h (Figure 7). Encapsulation efficiency was found to be 78.5%, 65.2%, and 51.3% for DRN-CNPs – 1, 2, and 3, respectively. Loading efficiency and % yield of DRN-CNPs-1 were found to be 13.8% and 35.7%, respectively (Table 3). Physical characteristics of DRN-CNPs were assessed by XRD technique and XRD-diffractogram is presented in Figure. 4.2θ peaks of DRN-CNPs were found to be at 28.94, 27.18, and 29.82. FWHM of these 2θ peaks was found to be 1.21, 0.68 and 0.12. Debye-Scherrer equation was applied to calculate the average size of NPs which was found to be 30.50nm (Figure 8) (Table 4). The IC_{50}values against MCF-7 cell lines for DRN and DRN-CNPs-1were found to be 30.21 and 25.46 respectively. Anticancer activity was dose dependent in both treatments and DRN-CNPs-1 was found to be more effective than DRN (Figure 9).

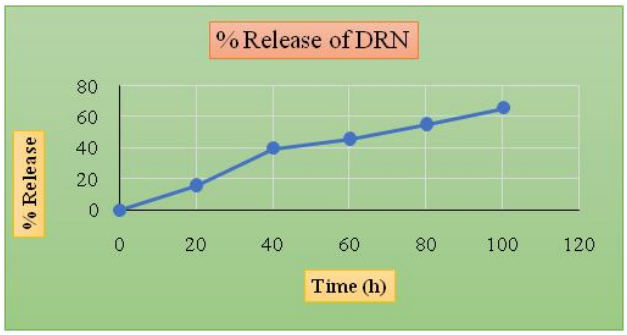

Figure 7: Percentage release of DRN from DRN-CNPs-1 at different time intervals.

Table 3: Encapsulation efficiency, loading efficiency, % yield of different DRN-CNPs formulations.

Formulation	EE%	LE%	% Yield
DRN-CNPs - 1	78.5	13.8	35.7
DRN-CNPs - 2	65.2	11.4	26.3
DRN-CNPs - 3	51.3	10.7	20.9

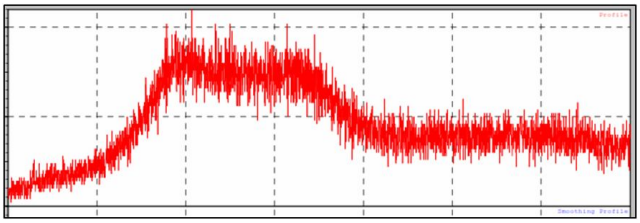

Figure 8: XRD of DRN-CNPs-1.

Table 4: 2θ peaks, FWHM, average particle size calculated from XRD of DRN-CNPs-1.

2-theta (deg)	FWHM beta (deg)	(Beta)	cos theta	D	Average
28.945	1.21	0.021118	0.968268	7.106882897	
27.18	0.68	0.011868	0.972002	12.59748624	30.50302
29.82	0.12	0.002094	0.966331	71.80467714	

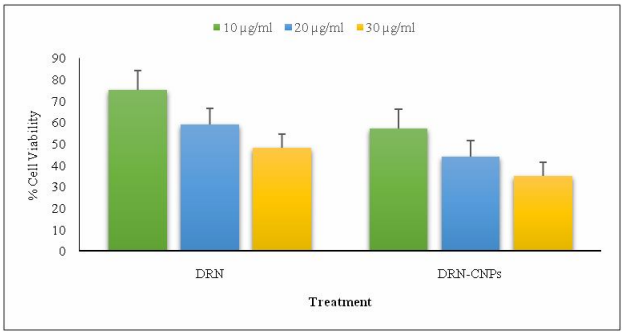

Figure 9: Percentage cell viability calculated for DRN and DRN-CNPs-1 against MCF-7 cells in MTT assay.

4. Discussion

Cancer remains a major challenge for mankind. Continuous research throughout the globe with all possibilities is focused to obtain complete cure and in large to decrease the annual mortality rate. Nanotechnology evolved as a boon not only to the scientific community but also to the people around the world. It is increasing the therapeutic efficacy of plant-based drugs having natural origin (Imad Uddin *et al*., 2019; Prairna *et al*., 2021; Naba *et al*., 2021) and also synthetic drugs having laboratory origin (Imad Uddin and Veeresh, 2020). DRN is one of the widely used anticancer drugs. It is the first option for the treatment of breast cancer. But, its usage is minimized due to increased multidrug resistance and cardiotoxicity (Mansoori *et al.*, 2017). Drug repurposing can be achieved by addressing these problems. DRN is a red color drug with high solubility in water. By using water as a solvent, further UV-based analysis was conducted to obtain Žmax (232 nm). Similar results are reported with Ye *et al.* (2015). In FTIR analysis, functional groups reported corresponds to DRN. A peak at 1729.31 cm^{-1} is reported for C=O stretching vibrations of DRN, this characteristic peak is also reported at a very near value of 1727 cm^{-1} by Hami *et al.* (2017). DRN peaks at 1070.59 cm^{-1} and 842.95 cm^{-1} are corresponding to peaks for CO_3^{2-}, similar peaks (1083 and 851 cm^{-1}) are earlier reported by Danmaigoro *et al.* (2017). The peak of chitosan at 3449.16 cm^{-1} corresponding to N-H & O-H stretching is also reported in the study conducted by Fernandes *et al*. (2015). Different peaks of chitosan, *viz.*, 2875.64, 1651.48, 1370.68 cm^{-1}, are other characteristic peaks. 2875.64 cm^{-1} is a characteristic peak of polysaccharides which is also reported in other polysaccharides (Melo-Silveira *et al.*, 2012). Characteristic peaks of STTP reported in our study are very close to FTIR peaks reported in a study conducted by Tomaz *et al.* (2018). In a physical mixture of both chitosan: STTP and DRN: chitosan: STTP characteristic peaks of all in the respective drugs is shown.

Successfully characterized drugs are now used for the preparation of a range of PLN-CNPs and DRN-CNPs to optimize the suitable concentration of chitosan, STTP, and DRN. For preparing PLN-CNPs volume of STTP added increased from formulation 1 to formulation 5. It was found that particle size and PDI decreased up to PLN-CNPs-3 and later on, it increased in PLN-CNPs 4 and 5. PLN-CNPs-3 showed a particle size of 716 nm and this was increased to 830 nm in DRN-CNPs-1. This increase in size is mostly due to the incorporation of DRN. A similar range of particle size for drug loaded chitosan NPs is reported in a study where 6-gingerol was used (Imad Uddin *et al*., 2020). PDI values are used to describe the distribution of molecular weight. So, as the concentration of DRN increased from formulation DRN-CNPs-1 to DRN-CNPs-3 there is an increase in the values of PDI indicating the broader molecular weight of formulation DRN-CNPs-3. However, an increase in particle size and high PDI are some of the disadvantages of the ionic gelation method (Das *et al*., 2019). The ZP, a measure of stability for formulation PLN-CNPs-3 was found to be -41.4 mV. Thereafter in the next formulations, it was decreased up to -28.7 mV. Whereas in the case of DRN-CNPs, ZP was decreased from formulation 1 to 3 with the highest value of 33.4 mV. These values of ZP indicate good stability of DRN-CNPs. As Mahobia *et al*. (2016) reported that values more than +25 mV or less than –25 mV have high degrees of stability. Electrophoretic mobility is measured by dividing electrophoretic velocity by electric field strength. This may be negative or positive. A negative sign indicates a moment of particles against to electrophoretic field. These values may decrease with an increase in the size of particles (Catherine, 2014). Our results are in accordance with this context, as EMM was least for PLN-CNPs-3 (-0.000124) when compared to other PLN-CNPs formulations. Thus, PLN-CNPs-3 is used for the synthesis of DRN-CNPs. Among these DRN-CNPs, first formulation, *i.e.*, DRN-CNPs-1 was found to be best suited for further studies.

In FTIR analysis, PLN-CNPs showed a single broad peak at 3273.96 cm^{-1}. A similar peak was also reported in another study conducted by Imad uddin *et al*. (2020). Whereas peak found at 3444.98 cm^{-1} in DRN-CNP-1 was also reported in a study conducted by Songsurang *et al*. (2011), where authors increased delivery of DRN by formulating them in chitosan NPs. There was a shift in peaks of DRN in DRN-CNPs-1, this indicates the loading of DRN in NPs. A peak at 1641.48 cm^{-1} in DRN-CNPs-1 was also reported in another study where DRN was loaded in iron oxide NPs (Norouzi *et al.*, 2020). The size of PLN-CNPs and DRN-CNPs was almost same and a similar range was reported byYousefpour *et al.* (2011).

Release of drug from DRN-CNPs-1 was calculated by dialysis bag method. In this method, NPs are embedded in a dialysis bag and the free drug moves out of the dialysis membrane because there is a concentration gradient of free drug between solvent inside and outside the dialysis bag (Yue *et al*., 2009). In a study, conducted by Zare *et al.* (2018), the percentage release of drug was found to be 30% (100 h) at pH 7.4, whereas in our study, release of drug was found to be 65% by 100 h at the same pH of 7.4. encapsulation and loading efficiency of DRN-CNPs-1 was found to be 78.5% and 13.8%, respectively. These results depict the successful development of DRN-CNPs. Encapsulation efficiency results are very close to the results of a study conducted by Fan *et al.* (2018), where DRN was encapsulated for the treatment enhancement of hepatocellular carcinoma. Rouhollah *et al.* (2013) calculated the loading efficiency of DRN in dendrimer coated magnetic NPs as 20%. Our results are also in the same pattern as this study with a loading efficiency of approximately 14%. In the XRD characterization technique, successful encapsulation of DRN in NPs is studied. 2è peak of 16.75 represents DRN (Chai *et al*., 2017), this peak was disappeared in DRN-CNPs-1, indicating successful incorporation of DRN in NPs. These successfully characterized DRN-CNPs-1 are compared for their increased antitumor activity against unloaded DRN by using MCF-7 cell lines in MTT assay. This assay is very commonly applied to evaluate the cellular metabolic activity by measuring cell viability, proliferation and

cytotoxicity (Riss *et al.*, 2019). The number of cells viable is 75%, 59%, and 48% at DRN concentrations of 10, 20, and 30 µg/ml. Whereas in DRN-CNPs-1, 57%, 44%, and 35% are the percentage cell viable at 10, 20, and 30 µg/ml. In both treatments, action produced was dose dependent and DRN-CNPs-1 was found to be more effective than DRN. Similar results are reported by Yousefpour *et al.* (2011). In our study, IC_{50} values for DRN and DRN-CNPs were found to be 30.21 and 25.46, respectively.

5. Conclusion

Cancer is a leading cause of death worldwide needs emergent attention. Among various types, breast cancer is the most prevalent. DRN is commonly used for the treatment of breast cancer. But, the use of the drug is minimized due to severe adverse effects and compromised cellular availability. To increase the efficiency of DRN, the present study was conducted. Different techniques like FTIR, SEM, are used to characterize synthesized NPs. These results supported the formation of DRN-CNPs. These NPs are also tested for the percentage of drug released at pH 7.4, encapsulation efficiency, loading efficiency, and % yield. Results of XRD, particle size estimation, and zeta potential measurement also proved the formation of NPs. Finally, antitumor efficacy was found to be more in DRN-CNPs than unloaded DRN. The assay was conducted by using an MCF-7 cell line. This research put forth an idea to use chitosan a biocompatible polymer for loading anticancer drugs like DRN to decrease their dose dependent adverse effects and increase their efficacy.

Conflict of interest

The authors declare no conflicts of interest related to this article.

References

American Cancer Society. Cancer Treatment and Survivorship Facts and Figures 2019-2021.(2019). Atlanta: American Cancer Society. Accessed on 04-12-2021. Available from: https://www.cancer.org/content/dam/cancer-org/research/cancer-facts-and-statistics/cancer-treatment-and-survivorship-facts-and-figures/cancer-treatment-and-survivorship-facts-and-figures-2019-2021.pdf

Catherine, C. (2014). Chapter E-Electrophoretic Mobility. Drioli, E. and Giorno, L. (eds.). Encyclopedia of Membranes. Springer-Verlag Berlin, Heidelberg.

Chai, F.; Sun, L.; He, X.; Li, J.; Liu, Y.; Xiong, F.; Ge, L.; Webster, T.J. and Zheng, C. (2017). Doxorubicin-loaded poly (lactic-co-glycolic acid) nanoparticles coated with chitosan/alginate by layer technology for antitumor applications. Int. J. Nanomedicine, **12**:1791-1802.

Chatterjee, K.; Zhang, J.; Honbo, N. and Karliner, J.S. (2010). Doxorubicin cardiomyopathy. Cardiology, **115**(2):155-162.

Danmaigoro, A.; Selvarajah, G.T.; Noor, M.H.M.; Mahmud, R.; Zakaria, M. and Bakar, Z.A. (2017). Development of cockleshell (Anadaragranosa) derived $CaCO_3$ nanoparticle for doxorubicin delivery. J. Comput. Theor. Nanos., **14**(10):5074-5086.

Das, S.; Singh, V.K.; Dwivedy, A.K.; Chaudhari, A.K.; Upadhyay, N.; Singh, P.; Sharma, S. and Dubey, N.K. (2019). Encapsulation in chitosan-based nanomatrix as an efficient green technology to boost the antimicrobial, antioxidant and *in situ* efficacy of *Coriandrum sativum* essential oil. Int. J. Biol. Macromol., **133**:294-305.

Mahobia, S.; Bajpai, J. and Bajpai, A.K. (2016). An *in vitro* investigation of swelling controlled delivery of insulin from egg albumin nanocarriers. Iran J. Pharm. Res., **15**(4):695.

Fan, D.; Yu, J.; Yan, R.; Xu, X.; Wang, Y.; Xie, X.; Chaolian, L.; Yonghua, L. and Huang, H. (2018). Preparation and evaluation of doxorubicin-loaded micelles based on glycyrrhetinic acid modified gelatin conjugates for targeting hepatocellular carcinoma. J. Nanomater, pp:20-29.

Fernandes Queiroz, M.; Melo, K.R.T.; Sabry, D.A.; Sassaki, G.L. and Rocha, H.A.O. (2015). Does the use of chitosan contribute to oxalate kidney stone formation? Marine drugs, **13**(1):141-158.

Hami, Z.; Rezayat, S.M.; Gilani, K.; Amini, M. and Ghazi-Khansari, M. (2017). *In vitro* cytotoxicity and combination effects of the docetaxel-conjugated and doxorubicin-conjugated poly (lactic acid)-poly (ethylene glycol)-folate-based polymeric micelles in human ovarian cancer cells. J. Pharm. Pharmacol., **69**(2):151-160.

Han, C.W.; De-Kuan, C. and Chia-Ting, H. (2006). Targeted therapy for cancer. J. Cancer Mol., **2**(2):57-66.

Imaduddin, M.D. and Veeresh, B. (2020). Systematic review on screening the role of chemosensitizer or synergistic drug and doxorubicin as dual drug loaded nanoparticle in overcoming multidrug resistant breast cancer. Ann. Phytomed., **9**(2):113-124. http://dx.doi.org/10.21276/ap.2020.9.2.9

Imaduddin, M.D.; Rachana, N.; Suraj, N.; Naveena, N. and Mounica, P. (2019). Screening anticancer activity of colchicine loaded chitosan nanoparticles. Pharmacophore, **10**(2):37-42.

Imaduddin, M.D.; Venkata Raja Srikar, P.; Preethi Karunya, Y.; Rachana, C. and Deepika, R. (2020). Synthesis and characterization of chitosan nanoparticles loaded with 6-gingerol isolated from *Zingiber officinale Rosc*. Ann. Phytomed., **9**(2):164-171.

Mansoori, B.; Mohammadi, A.; Davudian, S.; Shirjang, S. and Baradaran, B. (2017). The different mechanisms of cancer drug resistance: A brief review. Advanced Pharmaceutical Bulletin, **7**(3):339.

Melo-Silveira, R.F.; Fidelis, G.P.; Costa, M.S.S.P.; Telles, C.B.S.; Dantas-Santos, N.; Elias, S.O.; Ribeiro, V.B.; Barth, A.L.; Macedo, A.J.; Leite, E.L. and Rocha, H.A. (2012). *In vitro* antioxidant, anticoagulant and antimicrobial activity and in inhibition of cancer cell proliferation by xylan extracted from corn cobs. Int. J. Mol. Sci., **13**(1):409-426.

Naba, J.D.; Rita, N.; Shantanu, T.;Mousumi, H.; Seema, R.P. and Surjit, M.D. (2021). Green synthesis and characterization of silver nanoparticles using leaves extract of Neem (*Azadirachta indica* L.) and assessment of its *in vitro* antioxidant and antibacterial activity. Ann. Phytomed., **10**(1):171-177.

Norouzi, M.; Yathindranath, V.; Thliveris, J.A.; Kopec, B.M.; Siahaan, T.J. and Miller, D.W. (2020). Doxorubicin-loaded iron oxide nanoparticles for glioblastoma therapy: A combinational approach for enhanced delivery of nanoparticles. Sci. Rep., **10**:11292.

Othman, N.; Masarudin, M.J.; Kuen, C.Y.; Dasuan, N.A.; Abdullah, L.C.; Jamil, M. and Ain, S.N. (2018). Synthesis and optimization of chitosan nanoparticles loaded with l-ascorbic acid and thymoquinone. Nanomaterials, **8**(11):920.

Papac, R.J. (2001). Origins of cancer therapy. Yale J. Biol. Med., **74**(6):391-398.

Prados, J.; Melguizo, C.; Ortiz, R.; Vélez, C.; Alvarez, P.J.; Arias, J.L.; Ruíz, M.A.; Gallardo, V. and Aranega, A. (2012). Doxorubicin-loaded nanoparticles: new advances in breast cancer therapy. Anticancer Agents Med. Chem., **12**(9):1058-1070.

Prairna, B.; Shruti, S. and Ahmad, Ali. (2021). Potential activities of nanoparticles synthesized from *Nigella sativa* L. and its phytoconstituents: and overview. J. Phytonanotech. Pharmaceut. Sci., **1**(2):1-9.

Riss, T.; Niles, A.; Moravec, R.; Karassina, N. and Vidugiriene, J. (2019). Cytotoxicity Assays: *In vitro* methods to measure dead cells. In: Markossian, S.; Grossman, A.; Brimacombe, K.; Arkin, M.; Auld, D.; Austin, C.P.; Baell, J.; Chung, T.D.Y.; Coussens, N.P.; Dahlin, J.L.; Devanarayan, V.; Foley, T.L.; Glicksman, M.; Hall, M.D.; Haas, J.V.; Hoare, S.R.J.; Inglese, J.; Iversen, P.W.; Kales, S.C.; Lal-

Nag, M.; Li, Z.; McGee, J.; McManus, O.; Riss, T.; Saradjian, P.; Sittampalam, G.S.; Tarselli, M.; Trask, O.J.Jr.; Wang, Y.; Weidner, J.R.; Wildey, M.J.; Wilson, K.; Xia, M. and Xu, X. editors. Assay Guidance Manual [Internet]. Bethesda (MD): Eli Lilly and Company and the National Center for Advancing Translational Sciences, 2004.

Rouhollah, K.; Pelin, M.; Serap, Y.; Gozde, U. and Ufuk, G. (2013). Doxorubicin loading, release, and stability of polyamidoamine dendrimer-coated magnetic nanoparticles. J. Pharm. Sci., **102**(6):1825-1835.

Songsurang, K.; Praphairaksit, N.; Siraleartmukul, K. and Muangsin, N. (2011). Electrospray fabrication of doxorubicin-chitosan-tripolyphosphate nanoparticles for delivery of doxorubicin. Arch. Pharm. Res., **34**(4):583-592.

Tomaz, A.F.; de Carvalho, S.M.S.; Barbosa, R.C.; Silva, S.M.; Gutierrez, M.A.S.; de Lima, A.G.B. and Fook, M.V.L. (2018). Ionically crosslinked chitosan membranes used as drug carriers for cancer therapy application. Materials, **11**(10):2051.

World Health Organization. Cancer fact sheet 21 september 2021 (2021). Accessed on 04-12-2021. Available from: https://www.who.int/news-room/fact-sheets/detail/cancer

Yao, Y.; Zhou, Y.; Liu, L.; Xu, Y.; Chen, Q.; Wang, Y.; Wu, S.; Deng, Y.; Zhang, J. and Shao, A. (2020). Nanoparticle-based drug delivery in cancer therapy and its role in overcoming drug resistance. Front. Mol. Biosci., **7**:193:1-14.

Ye, W.L.; Zhao, Y.P.; Li, H.Q.; Na, R.; Li, F.; Mei, Q.B.; Zhao, M.G. and Zhou, S.Y. (2015). Doxorubicin-poly (ethylene glycol)-alendronate self-assembled micelles for targeted therapy of bone metastatic cancer. Sci. Rep., **5**(1):1-19.

Yousefpour, P.; Atyabi, F.; Vasheghani-Farahani, E.; Movahedi, A.A.M., and Dinarvand, R. (2011). Targeted delivery of doxorubicin-utilizing chitosan nanoparticles surface-functionalized with anti-Her2 trastuzumab. International Journal of Nanomedicine, **6**:1977-1990.

Yue, P.F.; Lu, X.Y.; Zhang, Z.Z.; Yuan, H.L.; Zhu, W.F.; Zheng, Q. and Yang, M. (2009). The study on the entrapment efficiency and *in vitro* release of puerarin submicron emulsion. Aaps. Pharmscitech., **10**(2):376-383.

Zare, M.; Samani, S.M. and Sobhani, Z. (2018). Enhanced intestinal permeation of doxorubicin using chitosan nanoparticles. Advanced Pharmaceutical Bulletin, **8**(3):411-417.

Zhang, Y.; Yang, C.; Wang, W.; Liu, J.; Liu, Q.; Huang, F.; Chu, L.; Gao, H.; Li, C.; Kong, D.; Liu, Q. and Liu, J. (2016). Co-delivery of doxorubicin and curcumin by pH-sensitive prodrug nanoparticle for combination therapy of cancer. Sci. Rep., **6**(1):1-12.

Citation **M.D. Imad Uddin and B. Veeresh (2021). An attempt to increase efficacy of doxorubicin against MCF-7 cells by using nanotechnology. Ann. Phytomed., 10(2):72-81. http://dx.doi.org/10.21276/ap.2021.10.2.10**